ELSEVIER

Journal of Photochemistry and Photobiology
A: Chemistry 85 (1995) 127–135

Journal of
PHOTOCHEMISTRY
AND
PHOTOBIOLOGY
A:CHEMISTRY

Fluorescence studies on a supramolecular porphyrin bearing anthracene donor moieties

Mallena Sirish, Bhaskar G. Maiya*

School of Chemistry, University of Hyderabad, Hyderabad 500 134, India

Received 10 March 1994; accepted 1 June 1994

Abstract

A tetraphenylporphyrin bearing four anthracene donor moieties (5,10,15,20-tetra(3-(9-methyloxyanthracenyl)phenyl)porphyrin, I) was synthesized and fully characterized. Spectroscopic and electrochemical data and results of metallation and intermolecular fluorescence quenching experiments suggest that there is no appreciable interaction between the porphyrin and anthracene moieties in I. Although intermolecular quenching of anthracene fluorescence by 5,10,15,20-(tetraphenyl)porphyrin is not obvious, the fluorescence of the anthracene donors in I is quenched by more than 90%. On the basis of the fluorescence excitation spectral data, the quenching observed is attributed to intramolecular singlet–singlet energy transfer from anthracene to the porphyrin. However, neither Förster's dipole–dipole formalism nor Dexter's electron exchange mechanism can explain adequately this intramolecular energy transfer. Thermodynamic considerations and solvent-dependent fluorescence data indicate that photoinduced electron transfer from singlet anthracene to the porphyrin can compete with energy transfer in this supramolecular system.

Keywords: Fluorescence; Porphyrins; Anthracene

1. Introduction

Although intramolecular singlet–singlet energy transfer has been examined in a large variety of covalently linked bis-porphyrin systems [1], only a few studies have dealt with energy transfer in porphyrins attached to other (rather than a porphyrin itself) donor hydrocarbon moieties [2–5]. In an attempt to mimic photosynthetic energy transfer reactions and to develop molecular devices, porphyrin systems, as energy acceptors, have been covalently linked to carotenoid [2,3], cyanine dye [4] and anthracene [5] donor subunits to form molecular dyads. The architectural symmetry of the porphyrin skeleton permits the attachment of more than one energy donor subunit, and such a supramolecular, light-harvesting system can be expected to show an antenna effect. Antenna systems comprising a central porphyrin linked to four peripheral porphyrin units have been reported [6–8]. Attempts have also been made to link four photon-harvesting hydrocarbon moieties to the porphyrin periphery. For example, naphthalene [9,10], anthracene [10,11], phenanthrene [12], pyrene [12] and pyrazole [13] groups have been linked directly to four *meso*-carbon centres of a porphin. In the last three cases, steady state fluorescence spectroscopy has indicated intramolecular energy transfer from the attached hydrocarbon units to the central porphyrin [13–15]. An analysis of the results described in all of these studies suggests that neither the attached hydrocarbon moiety nor the porphin itself retains its individual characteristics in these systems. In this sense, donor–acceptor (D–A) systems in which the energy donors are linked directly to the porphyrin periphery cannot be accurately described to possess an antenna function.

Thus it can be suggested that, in order to exhibit an antenna function, it is essential to have multicomponent structure in which the donors and acceptors retain their individual characteristics. The microstructure of such a supramolecular porphyrin should favour high local concentrations of the light-harvesting chromophores without forming intermolecular aggregates which are notorious energy-wasting sinks [16]. Furthermore, for a realistic description of the photosynthetic antenna function, a porphyrin-based model system should exhibit an electron transfer reaction in addition to an energy transfer reaction [2,17,18]. All of these considerations indicate that a molecular pentad system, in which a porphyrin acceptor is linked, via spacers, to four appropriately positioned donor hydrocarbons,

*Corresponding author.

SSDI 1010-6030(94)03893-Y

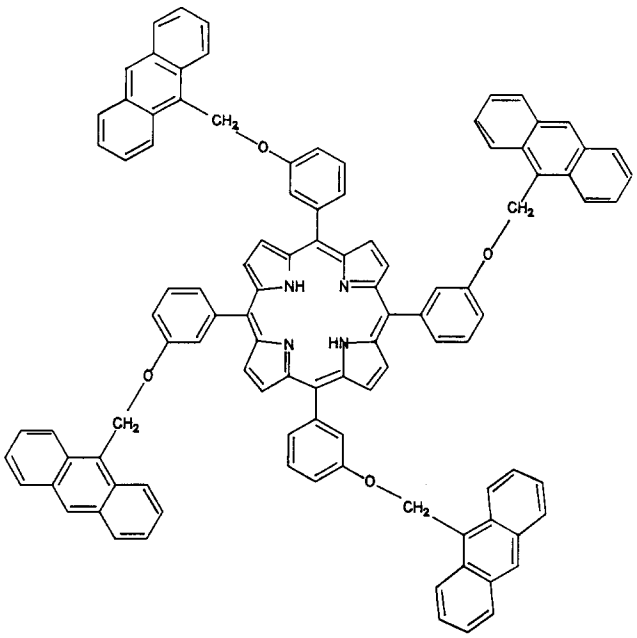

Fig. 1. Molecular structure of I.

forms a suitable choice for the demonstration of a biomimetic antenna function.

In this paper, we present results on a pentad system in which a 5,10,15,20-tetraphenylporphyrin (H_2TPP) is linked, via ether bridges, to four anthracene donor moieties (5,10,15,20-tetra(3-(9-methyloxyanthracenyl)-phenylporphyrin, a D_4–A pentad, **I**, Fig. 1). A detailed analysis of the spectroscopic, electrochemical and solvent-dependent fluorescence data indicates the occurrence of both energy and electron transfer reactions in this supramolecular porphyrin.

2. Experimental details

2.1. Materials

The solvents and all other common chemicals used in this study were purchased from BDH (India) and were purified according to standard procedures before use [19]. Pyrrole, *m*-hydroxybenzaldehyde and 9-chloromethylanthracene were purchased from Aldrich Chemical Company (USA). 5,10,15,20-Tetra(3-hydroxyphenyl)porphyrin (**II**) was synthesized as reported in Ref. [20].

5,10,15,20-Tetra(3-(9-methyloxyanthracenyl)phenyl)-porphyrin (**I**) was synthesized by condensing 1 mol equivalent of **II** with an excess of 9-chloromethylanthracene in dimethylformamide using potassium carbonate as a base. It was purified on an alumina column using $CHCl_3$–CH_3OH (10:1, v/v) as an eluent (yield, approximately 60%). The purity of the sample was checked by thin layer chromatography, analytical data and proton nuclear magnetic resonance (^1H NMR) methods. Analytical data: observed: C, 84.68%; H, 4.84%; N, 3.76%; calculated for $C_{104}H_{70}N_4O_4$: C, 86.60%; H, 4.87%; N, 3.88%. ^1H NMR ($CDCl_3$, tetramethylsilane (TMS)): δ_H (ppm) 8.96 (s, 8H; pyrrole), 8.45 (m, 10H; 1,8-anthryl and *o*-phenyl porphyrin), 7.98 (m, 14H; 4,5-anthryl and *m*- and *p*-phenyl porphyrin), 6.15 (s, 2H; $-OCH_2$, spacer), −2.76 (br s, 2H; –NH porphyrin).

Zinc(II) and copper(II) derivatives of **I** were prepared using procedures similar to that reported for the preparation of metallo derivatives of H_2TPP [21].

9-Methyloxyphenylanthracene (**III**) was synthesized by condensing phenol and 9-chloromethylanthracene; it was purified as described above for **I** (yield, approximately 80%). Melting point, 145 ± 2 °C. Analytical data: observed: C, 88.60%; H, 5.61%; calculated for $C_{20}H_{14}O$: C, 88.70%; H, 5.67%. ^1H NMR ($CDCl_3$, TMS): δ_H (ppm) 8.44 (s, 1H; 9-anthryl), 8.26 (m, 2H; 1,8-anthryl), 7.99 (m, 2H; 4,5-anthryl), 7.46 (m, 4H; 2,3,7,6-anthryl), 7.18 (m, 5H; phenyl), 5.96 (s, 2H; $-OCH_2-$).

2.2. Methods

UV–visible spectra were recorded with a Perkin–Elmer Lambda 3B spectrophotometer. Fluorescence spectra were recorded with a Hitachi model F-3010 spectrofluorometer employing right angle detection of fluorescence (slit widths, 2/2 nm (excitation/emission)). The concentrations of the samples were such that the optical absorbances at the excitation wavelengths (250 or 420 nm) were less than 0.2 for fluorescence spectra and about 10^{-7} M ($A_{420\ nm} = 0.02$) for fluorescence excitation spectra. A rhodamine 6G quantum counter was employed for spectral corrections (less than 600 nm). Fluorescence quantum yields (ϕ_f) were estimated by integrating the areas under the fluorescence curves and by using either H_2TPP (for excitation into the porphyrin band of **I**, 420 nm) or anthracene (for excitation into the anthracene band of **I**, 250 nm) as standards. The excitation spectra were overlapped with the absorption spectra after correcting for the instrument response function and after normalizing the spectra in the 500–600 nm region. The excitation spectrum of H_2TPP may well (±5%) be overlapped with its absorption spectrum in the wavelength region 220–600 nm under these experimental conditions. Corrections (λ^2) were applied whenever the data obtained as wavelengths were converted into wavenumbers [22].

The ^1H NMR spectra were recorded with a Bruker NR-200 AF-FT NMR instrument. The electron paramagnetic resonance (EPR) spectra were taken on a JEOL JM-FE3X EPR spectrometer. Differential pulse voltammetric experiments were performed with a Princeton Applied Research (PAR) electrochemical work station. A highly polished platinum button working

electrode, a Pt wire counter-electrode and a saturated calomel electrode (SCE) as reference were employed. The SCE was separated from the deoxygenated bulk electrolytic solution by a fritted glass disc junction containing the solvent (CH_2Cl_2) and the supporting electrolyte (tetra-*n*-butylammonium perchlorate (TBAP)).

Metallation reactions were followed by monitoring the decrease in absorbance at the 515 nm band of the porphyrins and by employing pseudo-first-order conditions ([I] or $[H_2TPP]=5\times10^{-5}$ M; [zinc acetate]$=5\times10^{-4}$ to 5×10^{-3} M).

Care was taken to avoid direct, ambient light entry into the samples during all the measurements. Unless otherwise stated, all experiments were carried out at 293 ± 3 K.

3. Results and discussion

3.1. Ground state properties

The UV–visible spectrum of **I** (Fig. 2) shows bands due to porphyrin (400–650 nm) and anthracene (220–350 nm) absorption. The shapes and the derived extinction coefficients of the bands in this spectrum are similar to those of a solution containing 1 mol equivalent of H_2TPP and 4 mol equivalents of anthracene. Similarly, the ^1H NMR spectrum of **I** has been compared with the spectra of H_2TPP and **III**. The results suggest that, except for the spacer $-OCH_2$ protons (which are slightly deshielded for **I** in comparison with **III**), the peak positions of all the other protons in **I** are not altered significantly with respect to those of the corresponding protons in the constituent partners. Moreover, the EPR spectrum of the copper(II) derivative of **I** shows g and A values ($g_{\|}=2.204\pm0.001$, $g_{\perp}=2.033\pm0.001$, $A_{\|}^{Cu}=(199\pm4)\times10^{-4}$ cm^{-1}, $A_{\|}^{N}=(14\pm1)\times10^{-4}$ cm^{-1}) similar to those observed for CuTPP [23] ($g_{\|}=2.203\pm0.001$, $g_{\perp}=2.027\pm0.001$, $A_{\|}^{Cu}=(198\pm1)\times10^{-4}$ cm^{-1}, $A_{\|}^{N}=(14\pm1)\times10^{-4}$ cm^{-1}) (toluene, 100 ± 3 K). Fig. 3 gives a comparison of the differential pulse voltammograms of **I**, H_2TPP, anthracene and **III**. As can be seen, the redox potentials of **I** do not vary significantly from those of its individual components. The porphyrin part of **I** is oxidized and reduced at 1.08 ± 0.03 V and -1.19 ± 0.03 V respectively, and all four anthracene subunits are oxidized in a single step at 1.51 ± 0.04 V (the peak having a large current value in Fig. 3). Thus UV–visible, ^1H NMR, EPR and redox potential data of **I** suggest that there is no appreciable interaction between the porphyrin and the anthracenes in this complex. Therefore the microstructure around the porphyrin is sufficiently "porous" and is devoid of perturbations arising from either crowding of the four anthracene subunits or π–π interactions between the porphyrin and anthracenes.

The above proposition is further substantiated by metallation reaction kinetics, excited state intermolecular electron transfer kinetics of the porphyrin part of **I** and structure simulation studies employing molecular mechanics calculations. In CH_3OH–$CHCl_3$ (1:1, v/v) mixtures, the second-order rate constants for zinc(II) insertion into **I** and H_2TPP are 0.28 ± 0.03 M^{-1} s^{-1} and 0.35 ± 0.04 M^{-1} s^{-1} respectively. The bimolecular

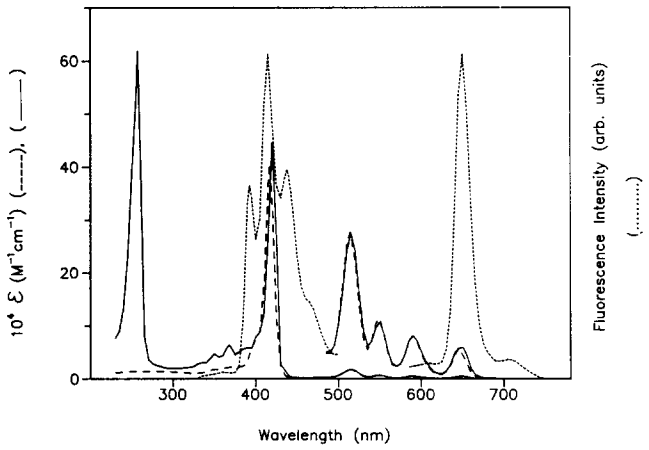

Fig. 2. UV–visible absorption spectra of H_2TPP (– – –) and **I** (——) and fluorescence spectra (· · · · ·) of **I** obtained on excitation at the anthracene (250 nm) absorption peak (emission range, 350–500 nm) and the porphyrin (420 nm) absorption peak (emission range, 580–750 nm). The solvent was CH_2Cl_2. The spectra were regenerated using absorption/fluorescence data obtained at 5 nm intervals.

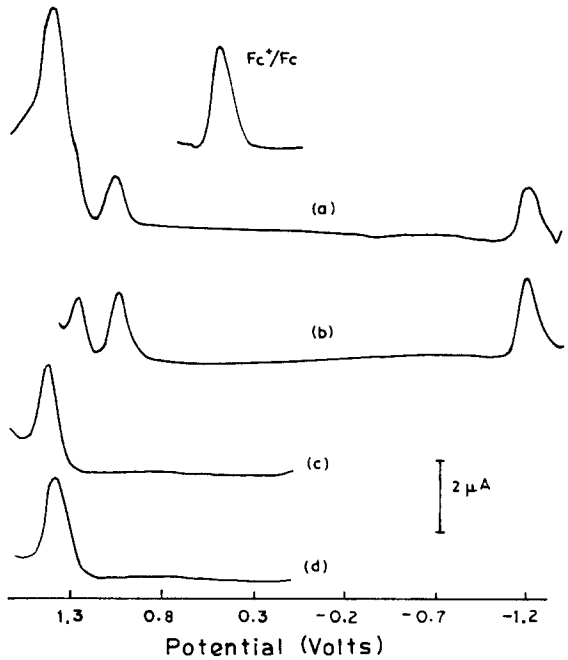

Fig. 3. Differential pulse voltammograms of **I** (a), H_2TPP (b), **III** (c) and anthracene (d) in CH_2Cl_2, 0.1 M TBAP (scan rate, 10 mV s^{-1}; modulation $\Delta E=10$ mV, modulation amplitude). The potential axis is referenced with respect to SCE. Fc, ferrocene.

rate constants (k_q) for steady state fluorescence quenching of **I** and H_2TPP (excitation at 420 nm where only the porphyrin part absorbs) by 2,4-dinitrobenzene (DNB) are $(4.3\pm0.4)\times10^9$ and $(5.4\pm0.6)\times10^9$ M^{-1} s^{-1} respectively (τ(**I**) = 8.02 ns and $\tau(H_2TPP)$ = 8.00 ns, λ_{exc} = 515 nm [24]). It has been proposed that quenching of H_2TPP by DNB involves a photoinduced electron transfer (PET) reaction [25], and the similarity between the k_q values observed for H_2TPP and **I** indicates that an intermolecular PET mechanism is also operative in the quenching of **I**. Thus both metallation and bimolecular fluorescence quenching experiments strongly indicate that the attached anthracene subunits do not physically hinder the approach of small molecules such as Zn^{2+} or DNB to the core porphyrin part of **I**. This situation is similar to that observed for a tetraporphyrin-substituted tetraphenylporphyrin [7]. Finally, molecular mechanics calculations (MMX, PCM4 model) and Corey–Pauling–Kaftun models suggest that the anthracene subunits are tilted away from the face of the porphyrin, thus avoiding mutual repulsions. The average centre-to-centre (CTC) distance, R, between the anthracenes and the porphyrin is 10.5 Å and the average dihedral angle encompassing $C_{3\text{-phenyl}}$–O–C_{CH_2}–$C_{9\text{-anthryl}}$ is $162\pm3°$.

3.2. Excited state properties

In methylene chloride solutions, excitation at either the porphyrin (420 nm) or anthracene (250 nm) band maximum of **I** gives the fluorescence spectra shown in Fig. 4. The corresponding fluorescence peak maxima are given in Table 1. The spectral shape and band maxima observed when **I** is excited at 420 nm are similar to the corresponding parameters for the fluorescence spectrum of H_2TPP. However the maxima of the fluorescence bands observed in the anthracene emission region of **I** (excitation at 250 nm) are slightly red shifted in comparison with the fluorescence band maxima of anthracene itself. That these red shifts are a consequence of substitution at the 9-position of anthracene in **I**, as was shown by fluorescence data obtained during previous studies on 9-substituted anthracene derivatives [26] and by the fact that the band maxima of **III** (392, 415 and 438 nm in CH_2Cl_2), a 9-substituted anthracene, occur at red-shifted wavelengths relative to those of anthracene (382, 403 and 427 nm in CH_2Cl_2). Nonetheless, from the overlap of the absorption and fluorescence spectra of **I** (see Fig. 2), the 0–0 spectroscopic transition energies ($E_{0\text{-}0}$) of the anthracene moiety (3.25 ± 0.05 eV) and porphyrin moiety (2.02 ± 0.05 eV) of the molecule are similar to the $E_{0\text{-}0}$ values of anthracene [27] and H_2TPP [28] respectively.

A major difference between the fluorescence data of **I** and those of anthracene lies in the magnitude of the ϕ_f values. Thus, although ϕ_f for excitation into the porphyrin moiety of the molecule (ϕ_f = 0.11) is similar to that for H_2TPP (ϕ_f = 0.11) [29] (see Fig. 4(b)), ϕ_f for excitation into the anthracene moiety of the molecule (ϕ_f = 0.012) is strongly quenched in comparison with the fluorescence of anthracene (ϕ_f = 0.24) [27] (see Fig. 4(a)). The quenching efficiency

$$Q = \frac{\phi_f(\text{anthracene}) - \phi_f(\mathbf{I})}{\phi_f(\text{anthracene})} \quad (1)$$

is 95% for **I** in CH_2Cl_2. The fluorescence spectra of **I** were also taken in hexane and CH_3CN, and the spectral data obtained in all three solvents are sum-

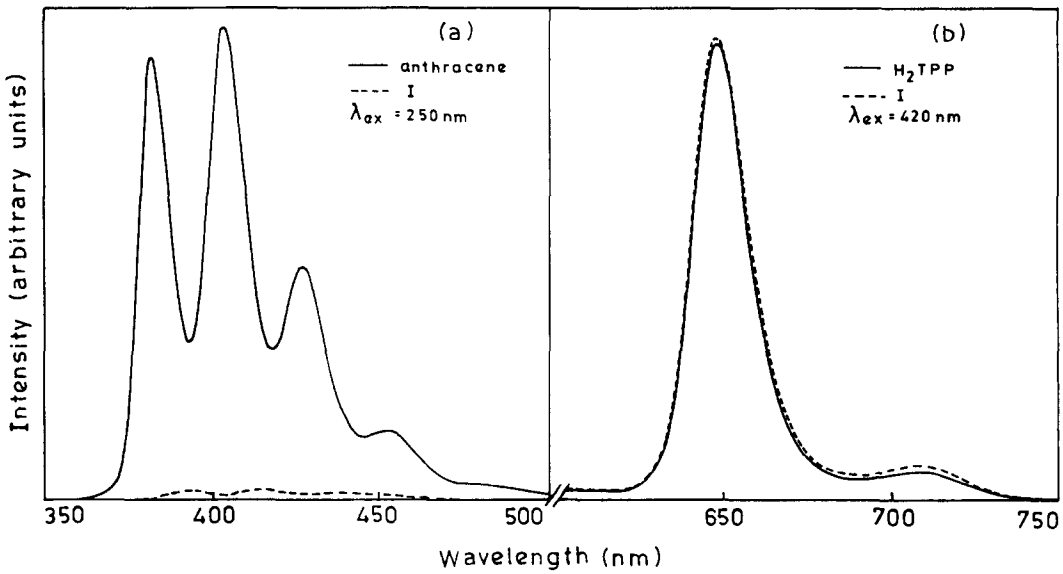

Fig. 4. Fluorescence spectra of equi-absorbing solutions (optical density (OD) at λ_{ex} = 0.11) of anthracene (——) and **I** (– – –) (λ_{ex} = 250 nm) (a) and H_2TPP (——) and **I** (– – –) (λ_{ex} = 420 nm) (b).

Table 1
Steady state fluorescence data of I[a]

Compound	Porphyrin band excitation (λ_{ex} = 420 nm)						Anthracene band excitation (λ_{ex} = 250 nm)					
	Hexane		CH_2Cl_2		CH_3CN		Hexane		CH_2Cl_2		CH_3CN	
	λ_{em} (nm)	ϕ_f	λ_{em} (nm)	ϕ_f	λ_{em} (nm)	ϕ_f	λ_{em} (nm)	ϕ_f	λ_{em} (nm)	ϕ_f	λ_{em} (nm)	ϕ_f
H_2TPP	650, 713	0.11	648, 708	0.11	648, 707	0.12						
Anthracene							377, 398, 421, 447	0.27	382, 403, 427, 452	0.24	379, 401, 424, 449	0.35
I	653, 713	0.11	648, 709	0.11	647, 707	0.11	388, 410, 434, 462	0.02	393, 413, 438, 466	0.01	391, 412, 436, 465	0.005

[a]Error limits: λ_{em}, ±1 nm; ϕ_f, ±5%.

marized in Table 1. An inspection of Table 1 suggests that anthracene fluorescence in I is quenched in all three solvents by more than 90% and that the percentage quenching efficiencies follow the order 99% (CH_3CN) > 95% (CH_2Cl_2) > 93% (hexane). It should be noted that this quenching is not due to the competitive absorption of incident light by the porphyrin part of I. This is because, at 250 nm, the contribution of porphyrin absorption is insignificant compared with the absorption due to the anthracene moieties in the molecule (compare the absorption data of I and H_2TPP at 250 nm in Fig. 2).

Fig. 2 also shows a considerable overlap between the emission of the anthracene moieties and the absorption of the porphyrin moiety in I. This suggests that the fluorescence quenching of the anthracene moieties in this compound may be due to intramolecular energy transfer from the excited singlet anthracenes to the porphyrin. Indeed, excitation of I at 250 nm results in the appearance of porphyrin emission bands in the 600–750 nm region in all three solvents. Furthermore, emission of both anthracene and porphyrin moieties is independent of the concentration of I. This observation not only shows that concentration quenching does not occur in I, but also rules out trivial reabsorption in this supramolecular complex.

Conclusive evidence for intramolecular singlet–singlet energy transfer comes from the excitation spectra. When emission is recorded at the porphyrin emission maximum (650 nm), the excitation spectrum of I shows bands characteristic of anthracene absorption. Fig. 5 shows an overlay of the corrected and normalized excitation spectra of I with the corresponding absorption spectra in the three solvents. A comparison of the excitation and absorption spectra in the 45.5×10^3 to 37.0×10^3 cm^{-1} (220–270 nm) region suggests energy transfer efficiencies (T_{obs}) of 76%±7%, 64%±6% and 36%±4% in hexane, CH_2Cl_2 and CH_3CN respectively. It should be noted here that, in each solvent, the T_{obs} values are lower than the Q values above and that opposite trends are obtained for T_{obs} ($CH_3CN < CH_2Cl_2 <$ hexane) and Q ($CH_3CN > CH_2Cl_2 >$ hexane) in this solvent series.

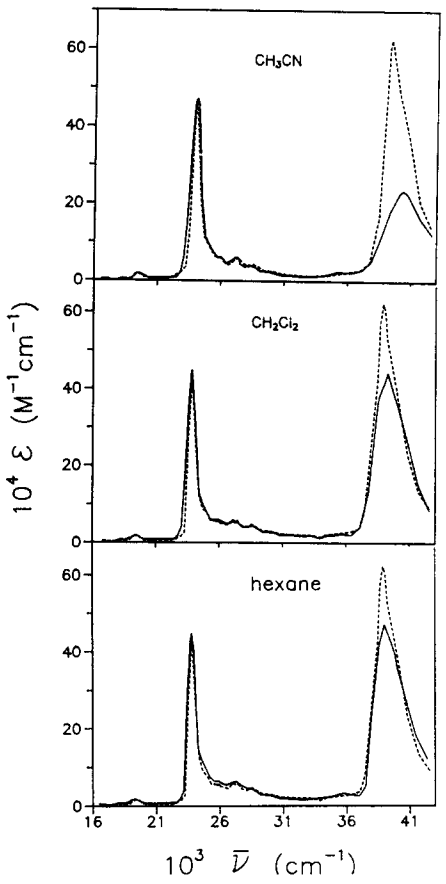

Fig. 5. Overlay of the excitation (——) and absorption (– – –) spectra of I in CH_3CN, CH_2Cl_2 and hexane (λ_{em} = 650 nm). The excitation spectra were corrected for the instrument response function and were normalized with respect to the absorption spectra between 16.6×10^3 cm^{-1} (600 nm) and 20.0×10^3 cm^{-1} (500 nm).

Intermolecular energy transfer between anthracene and H_2TPP is not obvious. The addition of 0.2×10^{-6} to 2×10^{-6} M of H_2TPP to a 1.0×10^{-6} M solution of anthracene results in an apparent decrease (by about 5%–10%) in fluorescence ($\lambda_{exc}=250$ nm) in the anthracene emission region and a concomitant progressive increase in fluorescence in the porphyrin emission region. Within experimental error, the increase in porphyrin emission observed in the presence of anthracene is the same as that obtained in the concentration-dependent (0.2×10^{-6} to 2.0×10^{-6} M) emission of H_2TPP ($\lambda_{exc}=250$ nm) in the absence of anthracene. Moreover, the excitation spectra ($\lambda_{em}=650$ nm) obtained for 4:1 and 1:1 (mol/mol) mixtures of anthracene and H_2TPP are indistinguishable from the spectrum obtained for H_2TPP alone. Collectively, these results suggest that the energy transfer efficiency between anthracene and porphyrin is more efficient in an intramolecular than an intermolecular situation.

Having noted the occurrence of intramolecular energy transfer in **I**, it is of further interest to investigate the possible mechanism(s) of energy transfer and to rationalize the opposite trends obtained for T_{obs} and Q values in the three solvents. In principle, singlet–singlet energy transfer can proceed either by Förster's dipole–dipole mechanism [30] or Dexter's electron exchange mechanism [31]. As most experimental observations of singlet–singlet transfer reactions in porphyrin-based D–A systems similar to **I** have been interpreted in terms of Förster's mechanism [2,4] we consider this first.

Key parameters obtained by analysing the energy transfer data of **I** using Förster's dipole–dipole formalism are summarized in Table 2. An inspection of this table suggests the following.

(1) The estimated critical energy transfer distances (R_0) are in the range 14.4–16.0 Å and the distances are somewhat longer than the CTC distance (R) in **I** (10.5 Å).

$$R_0=[8.8\times10^{23}\ k^2\phi_f(\text{anthracene})n^{-4}J_{\text{Förster}}]^{-6} \quad (2)$$

where

$$k^2=(\cos\gamma-3\cos\alpha\cos\beta)^2 \quad (3)$$

and

$$J_{\text{Förster}}=\int\bar{F}_D(\bar{\nu})\epsilon_A(\bar{\nu})\bar{\nu}^{-4}d\bar{\nu} \quad (4)$$

In Eq. (3), α and β are the angles made by the transition dipoles of anthracene and H_2TPP in **I** with a line joining the centres of the transitions, γ is the angle between the two transition dipoles and k^2 is the orientation factor. The value of k^2 was taken to be 0.66 assuming average orientation of the anthracenes with respect to the porphyrin plane in the excited state of **I**. We expect that this assumption is valid for **I** as both ^1H NMR and structure simulation studies (see above) show average orientation of four anthracenes around the porphyrin. In particular, the results do not indicate the presence of atropisomers (or rotamers) for **I** that are quite common for ortho-substituted tetraphenylporphyrins but not for meta-substituted tetraphenylporphyrins such as **I**. In Eq. (4), $\bar{F}_D(\bar{\nu})$ and $\epsilon_A(\bar{\nu})$ are the normalized fluorescence intensity of the donor (anthracene) and the molar extinction coefficient of the acceptor (H_2TPP) respectively. The estimated value of the overlap integral (donor emission and acceptor absorption), $J_{\text{Förster}}$, is $(2.64\pm0.2)\times10^{-16}$ cm^6 mmol^{-1}.

(2) Although the Q and T_{cal} values are similar, the T_{obs} values are consistently lower than both of these parameters in each solvent.

Table 2
Energy transfer data of **I**[a]

Solvent	n[b]	ϵ[b]	Q[c] (%)	R_0[d] (Å)	T_{cal}[e] (%)	T_{obs}[f] (%)	ΔG_{PET}[g] (eV)	k_{cal}^{En}[h] (10^9 s^{-1})	k_{obs}^{En}[h] (10^9 s^{-1})	k_{obs}[h] (10^9 s^{-1})	$k_{obs}-k_{obs}^{En}$ (10^9 s^{-1})
Hexane	1.375	1.88	93	15.6	91	76	−0.21	2.1	0.65	2.7	2.1
Methylene chloride	1.425	8.93	95	14.4	87	64	−0.70	1.3	0.34	3.7	3.4
Acetonitrile	1.344	37.50	99	16.0	92	36	−0.80	2.3	0.11	18.7	18.6

[a]Error limits: Q, ΔG_{PET} and k_{obs}, ±5%; R_0, T_{cal} and k_{cal}^{En}, ±7%; T_{obs} and k_{obs}^{En}, ±10%.

[b]n and ϵ are the refractive index and dielectric constant of the solvent respectively.

[c]Obtained using Eq. (1).

[d]Obtained using Eq. (2).

[e]Calculated using Eq. (5).

[f]Obtained from the overlay of the excitation spectrum of **I** normalized to its absorption spectrum (Fig. 5).

[g]$\Delta G_{PET}=E_{1/2}(ox)-E_{1/2}(red)-E_{0\text{-}0}+\Delta G_{Solv}$, where $\Delta G_{Solv}=e^2/2[(1/r_D)+(1/r_A)][(1/4\pi\epsilon_0\epsilon)-(1/4\pi\epsilon_0\epsilon_r)]-e^2/4\pi\epsilon_0\epsilon R$. $E_{1/2}(ox)$ and $E_{1/2}(red)$ are the potentials for one-electron oxidation of the donor (anthracene) and one-electron reduction of the acceptor (porphyrin) moieties of **I** respectively, r_D (4.8 Å) and r_A (7 Å) are the radii of the radical ions of the donor and acceptor respectively and ϵ_r and ϵ are the dielectric constants of CH_2Cl_2 and other solvents respectively. It should be noted that the compound is insoluble in CH_3CN, 0.1 M TBAP in electrochemical experiments. It should also be noted that incorporation of solvent correction terms to low-polarity situations is rather risky and hence the values of ΔG_{PET} in hexane can be taken as only a rough estimate [32].

[h]k_{obs}^{En}, k_{cal}^{En} and k_{obs} were obtained using Eqs. (6), (7) and (8) respectively.

$$T_{cal} = (R_0/R)^6/[1 + (R_0/R)^6] \quad (5)$$

(3) Similarly, the observed energy transfer rate constants (k_{obs}^{En}) are lower than the calculated rate constants (k_{cal}^{En}) in each solvent.

$$k_{obs}^{En} = [T_{obs}/(1 - T_{obs})]/\tau(\text{anthracene}) \quad (6)$$

and

$$k_{cal}^{En} = (R_0/R)^6/\tau(\text{anthracene}) \quad (7)$$

where τ(anthracene) is the lifetime of free anthracene (4.9, 5.2 and 5.3 ns in hexane [27], CH_2Cl_2 [24] and CH_3CN [27] respectively). Moreover, the k_{obs} values that are calculated on the basis of the quenching efficiencies are higher than both k_{cal}^{En} and k_{obs}^{En} in each solvent.

$$k_{obs} = [Q/(1 - Q)]/\tau(\text{anthracene}) \quad (8)$$

(4) The T_{obs} (k_{obs}^{En}) values bear no obvious relationship with the refractive index (n) of the solvent.

The above analysis indicates that quenching of the anthracene fluorescence in I is not entirely due to excitation energy transfer by Förster's dipole–dipole mechanism. This is substantiated by the fact that the T_{obs} (k_{obs}^{En}) values are consistently lower than the T_{cal} (k_{cal}^{En}) and Q (k_{obs}) values and there is no obvious correlation between T_{obs} (k_{obs}^{En}) and n values [30]. Possibly, other mechanism(s) may also be operative in the observed fluorescence quenching of I.

The estimated edge-to-edge approach distance between the anthracene and porphyrin in I is less than 6 Å (MMX calculations) and this may facilitate D–A orbital interactions, thus promoting Dexter's exchange process [31]. Dexter's mechanism involves both the lowest unoccupied molecular orbitals (LUMOs) and highest occupied molecular orbitals (HOMOs) of the donor and acceptor, and electron exchange can occur in either a concerted process or via stepwise electron transfer reactions involving radical intermediates (D^+A^-, D^-A^+). In this regard, it can be argued that if neither electron transfer step can occur to an orbital at a higher energy level, the HOMO and LUMO of the acceptor must either be isoenergetic with or sandwiched between the levels of the HOMO and LUMO of the donor. The latter situation is found to hold good for I as shown by the energy level diagram given in Fig. 6(a). It can be seen that the porphyrin energy levels (P^+ and P^-) are sandwiched between those of anthracene (A^+ and A^-) and that electron exchange energy transfer from singlet anthracene to the porphyrin subunit in I is possible on thermodynamic grounds. Thus both the distance and thermodynamic criteria indicate the possibility of the involvement of electron exchange energy transfer in I. This situation is similar to that observed by Lindsey et al. [4] in their studies on covalently linked porphyrin–cyanine dye dyads. This

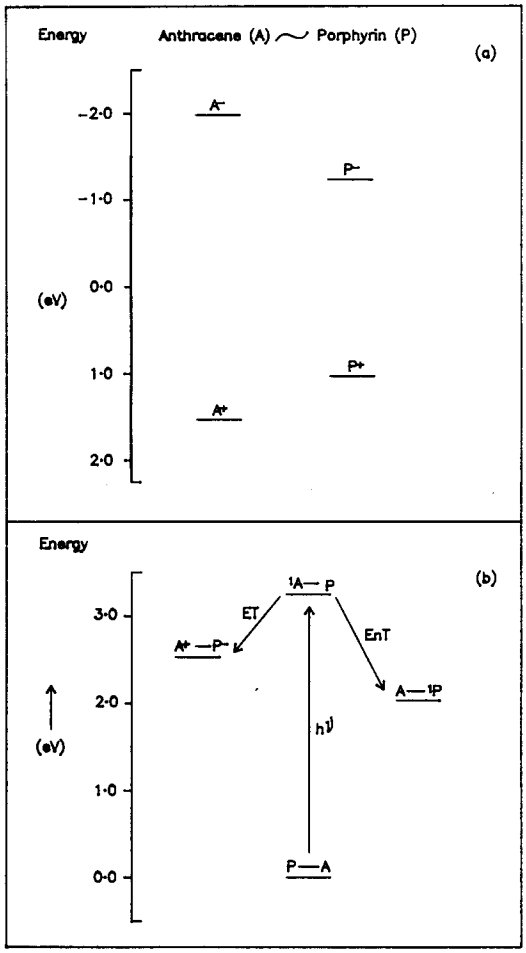

Fig. 6. (a) Energy levels of porphyrin (P) and anthracene (A) as derived from the electrochemical redox potential data of I. The reduction potential data of anthracene were taken from Ref. [33]. (b) Energy level diagram showing both energy (EnT) and electron (ET) transfer reactions from the singlet excited state of the anthracene moieties of I. The A^+–P^- state positioned in the figure is in CH_2Cl_2 and is sensitive to a change in solvent (see Table 2).

simple concept, however, must be tested further using a variety of D–A pairs with a prior knowledge of the orbital interactions involved. Our knowledge of D–A orbital interactions in I is limited at the present time. Nonetheless, the application of Dexter's theory does not rationalize why T_{obs} values are much lower than Q values for I in each solvent nor the opposite solvent dependence shown by these two parameters.

The data given in Fig. 6 clearly indicate the possibility of a PET reaction from singlet anthracene (A*) to the porphyrin (P) in I

$$A^*\text{–}P \longrightarrow A^+\text{–}P^- \quad (9)$$

The free energy changes for the above PET reaction (ΔG_{PET}) have been estimated in the three solvents used in this work (Table 2). The ΔG_{PET} values in CH_3CN and CH_2Cl_2 are highly exoergic and are close to the

energy difference between the singlet states of anthracene and porphyrin (approximately 1.2 eV, see Fig. 6(b)). Thus, under favourable conditions, a PET reaction can contribute to the quenching of anthracene emission in **I**, generating the A^+–P^- state (oxidative quenching). Considering the charge transfer nature of the process, ϵ of the medium is expected to influence the PET reaction efficiency. Inspection of Table 2 indicates that the estimated PET rate constants ($k_{obs} - k_{obs}^{En}$) correlate with ϵ of the solvent (this analysis assumes that the rates of the non-radiative processes of anthracene do not alter on attachment to the porphyrin in **I**). Moreover, as mentioned earlier, the Q (k_{obs}) and T_{obs} (k_{obs}^{En}) values show opposite trends with ϵ of the solvent. Collectively, these observations can be rationalized in terms of competition between energy transfer and electron transfer reactions in **I** (Fig. 6(b)), the electron transfer pathway taking over with an increase in the polarity of the medium.

Another type of electron transfer pathway, which involves a reductive quenching mechanism generating an A^-–P^+ charge transfer state, can also be envisaged to explain the quenching of anthracene fluorescence in **I**. However, there is some uncertainty involved in obtaining an accurate ground state reduction potential of the anthracene moiety of the molecule (Fig. 6(a)) and hence we shall not attempt to elaborate on this mechanism. Furthermore, it is also possible that the anthracene moieties in **I** may associate into a non-fluorescent excited state complex and that the amount of complex formation may be solvent dependent. In principle, this possibility can explain the additional quenching observed over and above that rationalized solely on the basis of energy transfer in **I**. Although this mechanism seems to be an attractive proposition, there are no spectral or other data to substantiate this viewpoint. Therefore we believe that the oxidative quenching mechanism described above certainly contributes to the low fluorescence quantum yield observed for the anthracene moieties in **I**.

Although there are a few reports in the literature describing the electron transfer reactions of covalently linked porphyrin–donor systems [34–37], reports discussing both energy and electron transfer reactions in such systems are scarce. In this regard, it should be noted that Moore and coworkers [17,18] have recently shown the possibility of both energy and electron transfer reactions in their porphyrin–carotene (P–C) dyads. Interestingly, the direction of the PET reaction in **I** (i.e. hydrocarbon → tetrapyrrole) is the same as that proposed previously for chlorophyll quenching by carotenoid [38,39] and that demonstrated recently for P–C dyads [17,18]. Clearly, studies on these kinds of supramolecular system are needed to obtain an understanding of the unexplored intricacies involved in the photosynthetic antenna function.

Acknowledgements

Thanks are due to the Council of Scientific and Industrial Research (CSIR, New Delhi, India) and the Department of Science and Technology (DST, New Delhi, India) for financial support of this work. We are grateful to Dr. T.P. Radhakrishnan for his help with the computational work and Dr. D. Birch (IBH Consultants, UK) for lifetime data. M.S. thanks the CSIR for a fellowship.

References

[1] S.G. Boxer, *Biochim. Biophys. Acta, 723* (1983) 965.
[2] D. Gust, T.A. Moore and A.L. Moore, *Acc. Chem. Res., 26* (1993) 198.
[3] A. Osuka, H. Yamada, K. Maruyama, N. Mataga, T. Asahi, M. Ohkouchi, T. Okada, I. Yamazaki and Y. Nishimura, *J. Am. Chem. Soc., 115* (1993) 9439.
[4] J.S. Lindsey, P.A. Brown and D.A. Siesel, *Tetrahedron, 45* (1989) 4845.
[5] F. Effenberger, H. Schlosser, P. Baverle, S. Maier, H. Port and H.C. Wolf, *Angew. Chem. Int. Ed. Engl., 27* (1988) 281.
[6] O. Wennerstrom, H. Erricsson, I. Ratson, S. Svensson and W. Pimlott, *Tetrahedron Lett., 30* (1989) 1129.
[7] J. Davila, A. Harriman and L.R. Milgrom, *Chem. Phys. Lett., 136* (1987) 427.
[8] S. Prathapan, T.E. Johnson and J.S. Lindsey, *J. Am. Chem. Soc., 115* (1993) 7519.
[9] R.J. Abraham, G.E. Hawkes, M.F. Hudson and K.M. Smith, *J. Chem. Soc., Perkin. Trans. II,* (1975) 204.
[10] H.N. Fonda, J.V. Gilbert, R.A. Cormier, J.R. Sprague, K. Kamioka and J.S. Connolly, *J. Phys. Chem., 97* (1993) 7024.
[11] J.M. Cense and R.-M. Le Quax, *Tetrahedron Lett., 39* (1979) 3725.
[12] A. Toeibs and N. Haeberle, *Justus Liebigs Ann. Chem., 718* (1968) 183.
[13] P. Suriyanarayanan and V. Krishnan, *Photochem. Photobiol., 38* (1983) 533.
[14] A. Harriman and J. Davila, *Tetrahedron, 45* (1989) 4737.
[15] Z.-M. Lin, W.-Z. Feng and H.-K. Leung, *J. Chem. Soc., Chem. Commun.,* (1991) 209.
[16] W.I. White, in D. Dolphin (ed.), *The Porphyrins,* Vol. V, Academic Press, New York, 1978, Chapter 7.
[17] D. Gust, T.A. Moore, A.L. Moore, C. Devadoss, P.A. Liddell, R. Hermant, R.A. Nieman, L.J. Demanche, J.M. DeGraziano and I. Gouri, *J. Am. Chem. Soc., 114* (1992) 3590.
[18] R.M. Hermant, P.A. Liddell, S. Lin, R.G. Alden, H.K. Kang, A.L. Moore, T.A. Moore and D. Gust, *J. Am. Chem. Soc., 115* (1993) 2080.
[19] D.D. Perrin, W.L.F. Armango and D.R. Perrin, *Purification of Laboratory Chemicals,* Pergamon, Oxford, 1986.
[20] R. Bonnett, S. Ioannou, R.D. White, U.-J. Winfield and M.C. Berenbaum, *Photobiochem. Photobiophys. Suppl.,* (1987) 45.
[21] P. Rothemund and A.R. Mennotti, *J. Am. Chem. Soc., 70* (1948) 697.
[22] J.R. Lackowicz, *Principles of Fluorescence Spectroscopy, Plenum, New York, 1983.*
[23] W.C. Lin, in D. Dolphin (ed.), *The Porphyrins,* Vol. IV, Academic Press, New York, 1978, Chapter 7.
[24] D. Birch, IBH Consultants, UK, personal communication of lifetime data, 1993.

[25] T.K. Chandrashekar and V. Krishnan, *Inorg. Chem., 20* (1981) 2782.
[26] A.K. Singh and M. Roy, *J. Photochem. Photobiol. B: Biol., 8* (1991) 325.
[27] S.L. Murov, *Handbook of Photochemistry,* Marcel Dekker, New York, 1973.
[28] M.A. Bergkamp, J. Dalton and T.L. Netzel, *J. Am. Chem. Soc., 104* (1982) 253.
[29] D.J. Quimby and F.R. Longo, *J. Am. Chem. Soc., 97* (1975) 5111.
[30] Th. Förster, *Discuss. Faraday Soc., 27* (1959) 7.
[31] D.L. Dexter, *J. Chem. Phys., 21* (1953) 836.
[32] M. Sirish and B.G. Maiya, *J. Photochem. Photobiol. A: Chem., 77* (1994) 189.
[33] C.K. Mann, *Electrochemical Reactions in Nonaqueous Systems,* Marcel Dekker, New York, 1970.
[34] A. Harriman and K. Hoise, *J. Photochem., 15* (1981) 163.
[35] M.R. Wasieleswski, G.L. Gaines III, M.P. O'Neil, W.A. Svec and M.P. Niemezyk, *J. Am. Chem. Soc., 112* (1990) 4559.
[36] G.R. Loppnow, D. Melamed, A.D. Hamilton and T.G. Spiro, *J. Phys. Chem., 97* (1993) 8957, and references cited therein.
[37] G.R. Loppnow, D. Melamed, A.R. Lehery, A.D. Hamilton and T.G. Spiro, *J. Phys. Chem., 97* (1993) 8969.
[38] G.S. Beddard, R.S. Davidson and K.R. Trethewey, *Nature, 267* (1977) 373.
[39] B. Demig-Adams, *Biochim. Biophys. Acta, 1020* (1990) 1.